

# *Microfabrication of 1-3 Composites with Photolithographically Defined Electrode Patterns for Kerfless Microultrasound Arrays*

Arjin Boonruang  
School of Engineering  
University of Glasgow  
Glasgow, Scotland, UK  
[2411978B@student.gla.ac.uk](mailto:2411978B@student.gla.ac.uk)

Tanikan Thongchai  
Faculty of Engineering  
Narasuan University  
Pitsanulok, Thailand  
[tanikant@nu.ac.th](mailto:tanikant@nu.ac.th)

Tim Button  
School of Metallurgy and  
Materials, University of  
Birmingham, UK  
[t.w.button@bham.ac.uk](mailto:t.w.button@bham.ac.uk)

Sandy Cochran  
School of Engineering  
University of Glasgow  
Glasgow, Scotland, UK  
[sandy.cochran@glasgow.ac.uk](mailto:sandy.cochran@glasgow.ac.uk)

**Abstract**— Microultrasound ( $\mu$ US) arrays are needed for biomedical imaging, especially for high definition subsurface diagnosis. Challenges of  $\mu$ US array development lie in ultrafine features of 1-3 piezocomposite structures and array elements to operate at 30 MHz. 1-3 piezocomposites with fine regular square and irregular pillars were fabricated using the dice-and-fill and gel-casting methods, respectively. Planar, parallel and smooth surfaces are required to achieve accurate size and good edge definition in photolithographically-defined array elements. Curing at elevated temperatures is also a consideration to provide environmental resistance for processing. After finishing to thickness, periodic thickness variation was found in the composites because of differences in the stiffnesses of ceramic and polymer. Average surface roughnesses of diced and randomised ceramic composite of 30 - 37 nm were achieved. Surface modification before electrode patterning was explored to promote good adhesion using plasma cleaning. The feasibility of patterning 20-element arrays with 50  $\mu$ m pitch on polished surfaces of 1-3 composites by photolithography is demonstrated.

**Keywords**—*Microultrasound, Microfabrication, Randomised Composite, Photolithography*

## I. INTRODUCTION

Microultrasound ( $\mu$ US) arrays operating at frequencies in the range from 30 MHz to over 50 MHz are required for high resolution biomedical imaging, with established uses in ophthalmology [1, 2], intravascular ultrasound [3, 4] and dermatology [5-7] and other uses emerging, e.g. ultrasound capsule endoscopy [8, 9]. Their primary benefit over conventional single element transducers (SET) is the capability for high-resolution imaging with extended depth of field from electronic scanning and focusing. Challenges in their development lie in the ultrafine features of the required composite structures and electrode arrays, in the order of 10  $\mu$ m. For example, a piezocomposite  $\mu$ US array operating at 30 MHz needs  $\sim$ 25  $\mu$ m pillar width,  $\sim$ 10  $\mu$ m of inter-pillar spacing, and pillar height of  $\sim$ 50  $\mu$ m to maintain an aspect ratio (height-to-width of ceramic pillar)  $AR = 2$  to produce adequate pulse response [10]. Additionally, ceramic volume fraction (CVF) up to 40% is required to maintain a high coupling coefficient [11].

Over the last decade, many methods including dice-and-fill technique [12, 13], injection moulding [14], laser machining [15], interdigital pair bonding [16], and viscous polymer processing (VPP) [10, 17, 18] have been developed to tackle this problem. However, limitations of these methods have also been found. Recently, 1-3 composites with irregular-shaped pillar for SETs operating at 30 MHz have been successfully fabricated by combining gel-casting with micromoulding. This approach can eliminate interference close to the operating frequency to achieve unperturbed thickness mode operation in simulation and practical results [18, 19]. Similarly, fine composite structures can also be achieved by a modified dice-and-fill method but without suppression of interference. This method is also necessary for  $\mu$ US arrays made with single crystal composite.

Another challenge in the development of  $\mu$ US arrays lies in the development of fine electrode arrays. Photolithography has been extensively used in microelectronic circuits because it provides electrode edge definition at the nanometre scale, controlled by the high spatial resolution of photoresist patterning. However, smooth and planar substrates are required. Many electrode patterns have been directly applied on flat Si substrates and bulk piezoelectric materials [12, 17, 20]. Fine electrode arrays have also been successfully patterned on highly smooth surfaces of 1-3 composites made with VPP by a bilayer lift-off photolithography process [21]. However, surface roughness must be considered because of systematic thickness variation observed in composite [22].

The objective of the work reported here is to advance innovative approaches explored previously in 1-3 piezocomposite designs, minimizing unwanted modes, whilst achieving necessary electrode patterns based on the use of photolithography for simple, kerfless array structures. These approaches demonstrate the feasibility of a manufacturing solution in development of composite and  $\mu$ US array fabrication.

## II. EXPERIMENTAL WORK

### A. 1-3 Piezocomposite Fabrication

1-3 piezocomposites have been designed and manufactured to demonstrate the feasibility of fabrication of fine-scale piezocomposite for  $\mu$ US arrays operating at  $f > 30$  MHz. The

---

This work was supported by The Royal Thai Government and Thailand Institute of Scientific and Technological Research (TISTR).

composites were made with ultrafine irregular-shaped pillars using a technique based on gel-casting and micromoulding, and, for comparison, regular square pillars using the dice-and-fill method, respectively.

Gel-casting, based on a near-net shape technique, requires dispersion of ceramic powders in a solution containing a monomer, crosslinker, initiator, and catalyst to form a low viscosity slurry. The solution is polymerised *in situ* and crosslinked to form a strong 3D-network of polymer to fix the dispersed ceramic particles in a mould. This technique can produce structures with high green strength (~ 50 MPa) prior to sintering. The casting requires replication of a soft mould (Polydimethylsiloxane: PDMS) which, in our case, was produced from a Si master mould defining a randomised composite pattern with 40% CVF [19].

A commercial PZT-5H type ceramic powder (TRS 610C, TRS Technologies, PA, USA) was mixed in a solution of an hydantoin epoxy resin (Hubei Xitai Chemical, China) and Bis (3-aminopropyl) amine (Sigma-Aldrich, Germany). The slurry, with 48 vol% solid loading and 30 wt% resin content, was cast into the soft mould, followed by demoulding. The green samples were sintered at 1200°C for 1 hr, then backfilled with epoxy (Epofix, Struers, UK).

Dice-and-fill has been widely used in many previous studies [13, 17, 23]. A sheet of PZ54 ceramic (Meggit AS, Kvistgaard, Denmark) was diced with a saw (DAD3320, Disco, Tokyo, Japan) with a nominal 10 µm blade (13 µm kerf), followed by backfilling with epoxy. At an operating frequency of 30 MHz, the fine-scale structure of the composite with a 38 µm pitch was accomplished by a modified dicing procedure, providing ~99% pillar survival and 43.7% CVF.

In the backfilling process, to prevent air entrapment in the kerfs, the samples were degassed for 20 minutes, followed by curing at 60°C for 2 hrs to enhance chemical and heat resistance by increasing crosslink density to raise the glass transition temperature of the epoxy [24]. This benefits the micro-fabrication process.

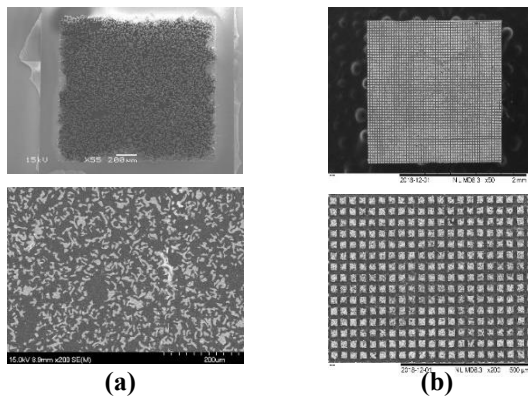


Figure 1. Top view of (a) irregular-shaped pillars before backfilling with 40% ceramic volume fraction (b) diced ceramic composite with 38-µm pitch and 43.7% ceramic volume fraction.

## B. Surface Preparation

Epoxy bumps were observed in the composites, particularly at the interface between the composite region and bulk epoxy because of differences in the mechanical properties of ceramic and polymer [21, 25]. Thickness variation between epoxy and ceramic pillar and surface roughness of a few µm can cause poor quality edge definition. Therefore, surface polishing was necessary after lapping to produce a parallel, smooth and flat composite substrate surface.

The surface preparation was performed with a PM5 lapping and polishing machine (Logitech, Glasgow, UK). Excess epoxy on the sample was lapped by solutions of 20 and 9 µm Al<sub>2</sub>O<sub>3</sub> powder (J-Mac Technologies, Glasgow, UK), followed by a solution of 3 µm powder to expose the pillars. The sample was then polished with colloidal silica polishing solution (SF1, Logitech, Glasgow, UK) on a polyurethane plate with a speed of 30 rpm. A minimum load of 750 g was applied for 1 hour.

## C. Microfabrication: Process Flow for Composite Substrates

Photolithography based on a bilayer lift-off process was utilized to define the array elements with 50-µm pitch. The generic procedure [21] is outlined in Table I. Depending on the material substrate, the process and recipe were optimized for different composite surfaces. In this study, positive photoresists LOR3A (MicroChem Corp., USA) and S1818 (MicroChem Corp., USA) were used. MF319 developer (MicroChem Corp., USA) was utilized to develop the undercut profile. After metallisation, the composites were immersed in 1165 stripper (MicroChem Corp., USA) to remove the remaining positive photoresist from sensitive substrate, then fine electrode arrays were created as shown in outline in Fig. 2. Various lift-off times were investigated on both composite substrates.

TABLE I. Process Flow

Process Step	Comments
1. Solvent cleaning by Spinning	Methanol, IPA and RO water.
2. LOR 3A spinning	A slow speed of 500 rpm for 5 secs was applied, then acceleration to 4000 rpm for 30 min.
3. LOR3A hot plate baking	150 °C for 5 min.
4. S1818 Spinning	A slow speed of 500 rpm for 5 sec was applied, then acceleration to 4000 rpm for 30 min.
5. S1818 hot plate baking	115°C for 3 min.
6. UV Exposure, hard contact	i-line, 365 nm.
7. Development	MIF319, 2.30 min.
8. Surface modification	Plasma Cleaning at 150 W for 1 min.
9. Metallisation	Ti/Au, thickness of 20/180 nm.
10. Lift-off in 1165 Stripper	1 - 2 hrs., followed by immersing in RO water for 5 mins, and blow drying.

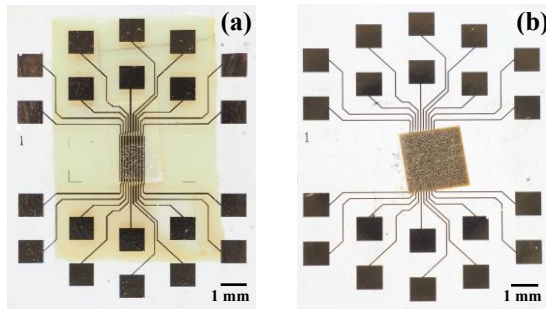


Figure 2. 50- $\mu\text{m}$  pitch test arrays with fan-out for  $\mu\text{US}$  arrays operating at 30 MHz patterned on (a) randomised composite (active area of  $1.6 \times 1.6 \text{ mm}^2$ ) and (b) diced composite (active area of  $2 \times 2 \text{ mm}^2$ ).

### III. RESULTS AND DISCUSSION

#### A. Functional Characterization of Composites

The aim of this section is to report investigation of the interference in impedance spectra that can cause poor biomedical imaging. Electrical impedance spectra were measured for randomised and diced ceramic composites using an impedance analyzer (4395A, Agilent Technologies Ltd., UK) with the results shown in Fig. 3. There was no evidence of spurious modes near an operating frequency at 30 MHz in the randomised composite, corresponding well with previous work [18, 19]. However, interference at 15 MHz was observed in the diced composite because of the periodicity of square pillars.

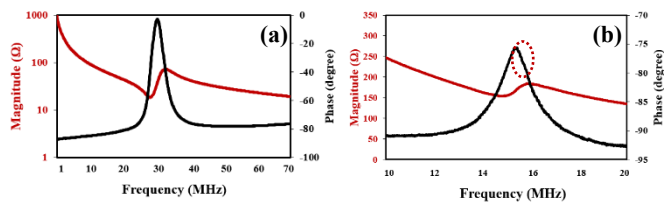


Figure 3. Electrical impedance spectra measured from composites (a) randomised (50- $\mu\text{m}$  thick) (b) diced ceramic (100- $\mu\text{m}$  thick) composites.

#### B. Surface Characterization of Composites

Thickness variation of ceramic pillars and epoxy was observed as shown in Fig 4. Thus, surface finishing is needed to provide a smooth surface prior to photolithography process. Surface roughnesses ( $R_a$ ) of 30 and 38 nm were achieved in diced and randomised ceramic composites, respectively. The difference in  $R_a$  can be explained by the load being absorbed by epoxy. The overall size of the epoxy coupons was  $11 \times 12 \text{ mm}^2$ , based on the size of the fan-out. However, the volume of the active area in the diced composites was larger than that of a randomised composite by 40%; the epoxy volume fraction in the former was less than the latter. Consequently, polishing of the active area in a diced composite was easier to accomplish than in a randomised composite, leading to better  $R_a$ .

#### C. Process Development for Composites

In the bilayer lift-off process, undercut profile was created as shown in Fig. 5(a). The undercut facilitates penetration of the 1165 stripper beneath the S1818 layer, so unexposed resist can

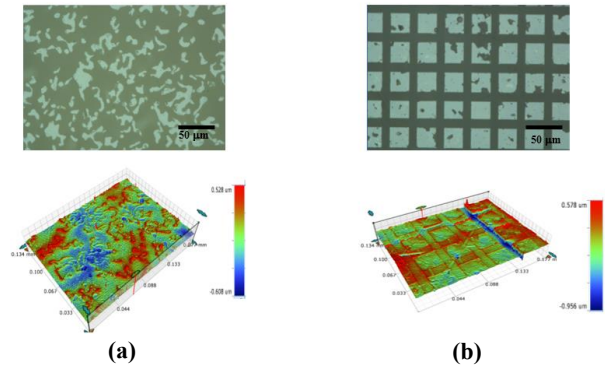


Figure 4. Optical microscopy and 3D imaging by optical profiling of (a) randomised and (b) diced composites.

be easily dissolved. Typically, LOR film should be thicker than the deposited metal film by 25% to provide clean lift-off and good edge definition, particularly in composites [26]. The LOR3A thickness was  $0.3 \mu\text{m}$  in this study, 33% thicker than the metal film.

An array pattern of exposed resist was successfully developed on both composites without evidence of residual resist as illustrated in Fig. 5 (b) and (c). Electrode arrays were properly patterned on both composite substrates as shown in Fig 6. However, a difference in lift-off time was necessary: in the diced composite, the lift-off time was 1.15 hrs to provide good edge definition.

The randomised composite required a longer lift-off time of 2 hrs to completely remove metal on unexposed resist as illustrated in Fig 7. This can be explained by stronger adhesion and connectivity of epoxy in the randomised composite. This can certainly be considered in the spacing between array elements because of metal on unexposed resist at the necessary fine spacing.

It was found that the area fraction of epoxy in the randomised composite (80%) was larger than that of the diced composite (50%) by 30%. This was because the former had pillar feature size, randomly ranging from 2-50  $\mu\text{m}$ , compared to the latter which had periodicity associated with a 25- $\mu\text{m}$  pillar width. The irregularity of pillar sizes and patterns increases the possibility of epoxy connectivity in the randomised composite. Another possible reason for the increased epoxy connectivity is through pillars destroyed during demoulding.

As a result, the randomised composite required more time in the lift-off process to entirely remove the metal film on unexposed resist. It can be seen that the shape of an element is dependent on the irregularity, but clean edge definition and proper array element sizing could be obtained successfully.

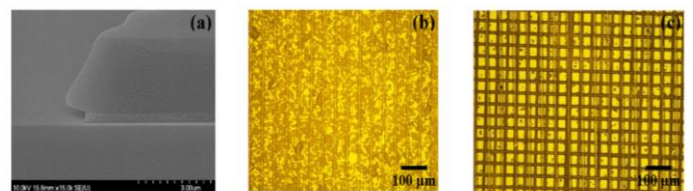


Figure 5. Profile of bilayer resist on (a) Si substrate, (b) randomised composite and (c) diced composite.

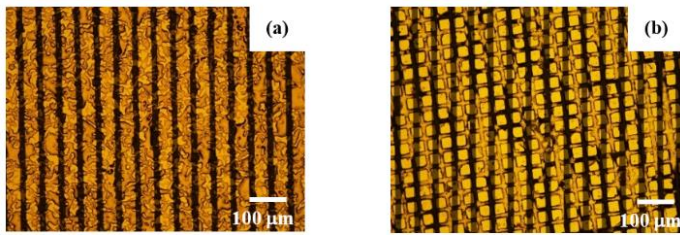


Figure 6. Optical images at 20x of 50- $\mu$ m pitch array elements patterned on (a) randomised composite (b) diced composite.

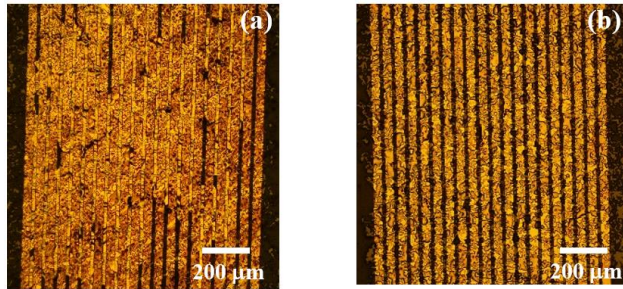


Figure 7. Optical photomicrographs of array elements patterned on randomised composites with lift-off times (a) 1.15 hrs and (b) 2 hrs.

#### IV. CONCLUSIONS

Randomised composites with lateral feature size range 2 - 50  $\mu$ m were fabricated using a gel-casting method together with micromoulding. Diced ceramic composites with a pitch of 38  $\mu$ m were achieved with ~99% pillar survival rate during the ultra-fine pillar dicing process. Epoxy curing at an elevated temperature was required to maximize resistance to parameters essential in the photolithography process. Thickness variation was observed in the composites due to differences in stiffness properties of the ceramic and polymer materials. Surface polishing was required which resulted in surface roughness, Ra, of 30 and 38 nm in diced and randomised ceramic composites. Electrodes defining 20 element arrays with 50  $\mu$ m pitch were patterned using a bilayer lift-off process on the polished surface of both composites. Satisfactory edge definition was achieved by process optimization on both composite substrates. A longer lift-off process time was found to be needed in the randomised composite due to a larger area and more adhesion of the epoxy.

#### ACKNOWLEDGEMENTS

The authors acknowledge the James Watt Nanofabrication Centre, University of Glasgow for clean room facilities, J.McAneny for his private communications, Dr. Y.Qiu and Dr. R.McPhillips for their contribution to the transducer fabrication process, and H.Thomson and B.Abaravicius for correction and reviewing of this MS. The Royal Thai Government is the PhD funder for A.Boonruang.

#### REFERENCES

[1] Coleman, D.J., et al., *Explaining The Current Role Of High Frequency Ultrasound In Ophthalmic Diagnosis (Ophthalmic Ultrasound)*. Expert Rev Ophthalmol, 2006. 1(1): p. 63-76.  
[2] Waldron, R.G., *B-Scan Ocular Ultrasound\_ Overview, Indications for Examination, Ultrasound Principles and Physics.pdf*. Medscape, 2016.

[3] Li, X., et al., *80 MHz Intravascular Ultrasound (IVUS) transducer*. IEEE International Ultrasonics Symposium Proceedings, 2011.  
[4] Vasquez, A., N. Mistry, and J. Singh, *Impact of Intravascular Ultrasound in Clinical Practice*. Coronary Diagnosis & Imaging, 2014.  
[5] Alfageme Roldán, F., *Ultrasound Skin Imaging*. Actas Dermo-Sifiliográficas (English Edition), 2014. 105(10): p. 891-899.  
[6] Kleinerman, R., et al., *Ultrasound in dermatology: principles and applications*. J Am Acad Dermatol, 2012. 67(3): p. 478-87.  
[7] Turnbull, D.H., et al., *A 40-100 MHz B-scan ultrasound backscatter microscope for skin imaging*. Ultrasound in Med. & Biol, 1995. 21(1): p. 79-88.  
[8] Cox, B.F., et al., *Ultrasound capsule endoscopy: sounding out the future*. Ann Transl Med, 2017. 5(9): p. 201.  
[9] Lay, H.S., et al., *Microultrasound characterisation of ex vivo porcine tissue for ultrasound capsule endoscopy*. Journal of Physics: Conference Series, 2017. 797.  
[10] Abrar, A., et al., *1-3 connectivity piezoelectric ceramic-polymer composite transducers made with viscous polymer processing for high frequency ultrasound*. Ultrasonics, 2004. 42(1-9): p. 479-84.  
[11] Aduld, W.A.S.a.B.A., *Modeling 1-3 composite piezoelectrics thickness-mode oscillations*. IEEE Trans. Ultrason. Ferroelectr. Freq. Control, 1991. 38(No. 1): p. 40-47.  
[12] Brown, J., et al., *Fabrication and performance of a 40-MHz linear array based on a 1-3 composite with geometric elevation focusing*. IEEE Transactions on Ultrasonics, Ferroelectrics, and Frequency Control, 2007. 54(9): p. 1888-1894.  
[13] Brown, J.A., et al., *Fabrication and performance of high-frequency composite transducers with triangular-pillar geometry*. IEEE Trans Ultrason Ferroelectr Freq Control, 2009. 56(No. 4): p. 827-836.  
[14] Bowen, L.J., et al., *Injection molded fine-scale piezoelectric composite transducers, in Ultrasonic Symposium*. 1993.  
[15] Farlow, R., et al., *Micromachining of a Piezocomposite Transducer Using a Copper Vapor Laser, in IEEE Trans Ultrason Ferroelectr Freq Control*. 2001.  
[16] Liu, R., K.A. Harasiewicz, and F.S. Foster, *Interdigital pair bonding for high frequency (20-50 MHz) ultrasonic composite transducers*. IEEE Transactions on Ultrasonics, Ferroelectrics, and Frequency Control, 2001. 48(1): p. 299-306.  
[17] Bezanson, A., R. Adamson, and J. Brown, *Fabrication and performance of a miniaturized 64-element high-frequency endoscopic phased array*. IEEE Transactions on Ultrasonics, Ferroelectrics, and Frequency Control, 2014. 60(1): p. 33-43.  
[18] Demore, C.E.M., et al., *1-3 piezocomposite design optimised for high frequency kerfless transducer arrays, in 2009 IEEE International Ultrasonics Symposium*. 2009. p. 1-4.  
[19] Y. Jiang, C.E.M.D., C. Meggs, C. Dunare, T. Stevenson, J. Bamber, S. Cochran, T.W. Button, *Micro-moulded Randomised Piezocomposites for High Frequency Ultrasound Imaging*. IEEE International Ultrasonics Symposium, 2012.  
[20] Golden, J., Miller, H., Nawrocki, D., Ross, J., *Optimization of Bilayer lift-off resist process, in CS MANTECH Conference*. 2009: Florida, USA.  
[21] Bernassau, A.L., et al., *Microfabrication of electrode patterns for high-frequency ultrasound transducer arrays*. IEEE Trans Ultrason Ferroelectr Freq Control, 2012. 59(8): p. 1820-9.  
[22] MacLennan, D., et al., *Ultra Precision Grinding in the Fabrication of High Frequency Piezocomposite Ultrasonic Transducers*. IEEE Ultrasonics symposium, 2006.  
[23] Yin, J., et al., *High-frequency piezo-composite transducer with hexagonal pillars*. IEEE International Ultrasonics Symposium Proceedings., 2009: p. 2750-2753. .  
[24] Petrie, E.M., *Epoxy Adhesive Formulations*. 2006: McGraw-Hill.  
[25] MacLennan, D., et al., *Ultra precise grinding in the fabrication of high frequency piezocomposite ultrasonic transducers*. IEEE Ultrasonics Symposium, 2006.  
[26] MicroChem, *LOR and PMGI Resists*. Accessed 10<sup>th</sup> September 2019, (<http://microchem.com/pdf/PMGI-Resists-data-sheet-V-rhcedit-102206.pdf>)